SEMARAK ILMU PUBLISHING

Journal of Advanced Research in Applied Sciences and Engineering Technology

Journal homepage:
https://semarakilmu.com.my/journals/index.php/applied_sciences_eng_tech/index
ISSN: 2462-1943

The Architecture of 3D Sensory Scanner System for Storing Shelf

Thinaharan Ramachandran[1], Sokchoo Ng[1,*], Vincent Tai[2], Yongchai Tan[2], Li Yanling[3]

[1] Faculty Arts and Science, International University of Malay-Wales, 50480 Kuala Lumpur, Malaysia
[2] Centre for Modelling and Simulation, Faculty of Engineering, Built Environment and Information Technology, SEGI University, 47810 Petaling Jaya, Selangor, Malaysia
[3] Artificial Intelligence College, Bao Ding University, 71 East 3027 Road, Bao Ding, Hebei Province, China

ARTICLE INFO

Article history:
Received 16 August 2023
Received in revised form 13 January 2024
Accepted 2 March 2024
Available online 4 June 2024

Keywords:
Shelf-tier; 3D; LiDAR; Tripod-scanner; Free-space

ABSTRACT

The storage shelves are available in different sizes for storing objects in different shapes, colours, sizes and surfaces. Many technologies are available for transforming human-intensive jobs into machines, such as robots handling picking, placing and sorting, but these robots need datasets to process and handle effectively. A distance sensor is suitable to measure distances between objects and to obtain free spaces that are available in a shelf tier. A Light Detection and Ranging (LiDAR) sensor can measure distances better than Ultrasonic (US) and Infrared distance sensors (IR) because it has good sensitivity to detect near and far objects. Spherical coordinates that are recorded from a LiDAR are transformed into cartesian coordinates to obtain a 3D impression of a shelf tier. This study aims to propose an effective 3D sensory scanning system to estimate the percentage of free space in a shelf tier by using cloud point data (CPD). The first step is to determine a suitable distance sensor that can be mounted on a tripod scanner to obtain CPD. The spherical datasets then were converted into cartesian coordinates. The motor speed was analysed with Pearson Correlation analysis to determine a suitable rotating speed to construct a 3D impression. Experimental results showed the designed scanner is capable to scan CPD at a suitable motor rotational speed, and with the 3D plot from cartesian coordinates, it is easy to distinguish between areas with and without objects in a shelf tier.

1. Introduction

Storage shelves are important for daily use in homes, offices and in manufacturing enterprises. The shelves are used for keeping objects in various sizes, shapes, surfaces and colours. It is a tedious process to estimate free spaces in a shelf tier because it is computationally challenging and more time is required for measuring and calculating the volume of every object before storing.

However, human being applies cognitive, perception and imaginative methods to solve complex object arrangements. In the future, machines will be handling most laborious jobs, like stocking, picking, placing, monitoring and cleaning. The machines need sufficient datasets for reasoning and processing action functions. A pick-place robot becomes versatile in arranging objects on a shelf if

* *Corresponding author.*
E-mail address: ashleyng@iumw.edu.my

https://doi.org/10.37934/araset.46.2.1025

the robot knows the available spaces. Distribution or production warehouses have a multi-story automatic shelf, but shelves do not come with alerting function to inform storekeepers about free spaces in a shelf [1]. A distance sensor is suitable for measuring the distances between objects, and by processing distance data is easier to determine the available free space. A distance sensor is eccentrically sensitive to temperature, humidity and position, so it is important to validate distance sensors for measuring distances for different applications. Although there are various types of machine learning algorithms to predict accurately, corrupted data harvested from a data acquisition system will be affecting the prediction accuracy.

2. Literature Survey

2.1 Automation Storage

An automated storage rack and retrieval system (AS/RS) has a higher density to utilise inventory spaces, from spending to rent or buying additional spaces for increasing storage capacity [2]. Manufacturers already start requesting rack builders to build dynamic shelves that can improve the goods delivery mechanisms because the yearly e-commerce business trend shows exponential growth [3]. There are processes like unloading, counting, identifying, quality control and final acceptance of goods area in a warehouse. When goods arrived, they are transferred to the holding bay and then moved to dedicated shelves for storage [4]. The operation issues in a warehouse can be solved with a smart automation environment. Put-away information is an essential picker list, but this process is expensive and will take 15% of the operation time in a warehouse. Almost 55% of operation time is absorbed by the warehouse employees while handling pick-list and processes like searching, extracting and recording data. As to conclude, each process in a warehouse takes time, consumes extra human resources, and uses bundles or papers for recording data, tracking and monitoring processes. Therefore, smarter processes are required to optimise productivity in a warehouse [5]. There is demand for designing automation shelves which exponentially revolutionizing. The pick and place system manipulate object orientation, but it has lesser spaces to pick items inside a shelf's tier. There is a pick-place system that relatively manipulates object orientation, but these shelves have lesser spaces to pick items inside a shelf's tier because these shelves are narrow, dark, and consist of multiple things [6].

2.2 Sensors

A high-definition camera captures clear images to extract features for tracking and detecting objects, however, brighter colours like vests will cause a distraction to images captured from a camera [7]. On the other hand, Light Detection and Ranging (LiDAR) sensor is another choice to obtain input signals for the predictive model to automatically prohibit vehicles from entering a restricted area than estimating from the unclear images. A camera detection decays under diverse weather conditions, especially during sunset which is causing darker and lesser contrasts [8]. LiDAR has been used in application development for detecting roads, especially suitable for places with marginal weather. LiDAR measures shorter with accurate distances between 10 to 100 meters [4]. Different types of distance sensors have different characteristics and detection ranges. For example, a distance sensor applied to a mobile robot estimates distances in obstacle paths. A microcontroller reads the sensor data and coordinates the moving path. Therefore, factors like sensor price, atmospheric conditions, obstacles characteristics, detection ranges and precision levels have to be considered in selecting a sensor [9]. The characteristic analysis between infrared, ultrasonic and laser sensors are the basis to determine the suitability sensor for its application [10]. An ultrasonic sensor uses Time

of Flight (ToF) in measuring distances between objects because the echo signals hit an object's surface and return the reflective signal in a definite time [11]. LiDAR sensor is preferable for 3D object detection in an autonomous vehicle as comparatively, point cloud data are more reliable and accurate than RGB images from video cameras. The point cloud data detect objects and describes shapes, but point cloud properties are unordered and sparsity, causing the challenge to detect an object directly from the point cloud [12]. Additional care is needed to position and mount a sensor otherwise a little change in the angle position will affect measurement values. An ultrasonic sensor has a wide beam for measuring the distances of reflective surface objects within 0.5 m. Measuring distances in an unknown environment using an IR sensor is a challenge, but combining an ultrasonic and IR sensor will compensate for the disadvantages to estimates accurate distance measurements [13]. An experiment was conducted with infrared sensors on a rig to construct a 3D image. Five infrared sensors mounted on a rotating rig at 2 degrees at each turn has reconstructed 3D impression of different shapes of prosthetic cone, but the IR sensor is sensitive to surrounding reflection e, especially reflecting objects. The experiment was conducted in a dark room and rotational angles were reduced for achieving accurate results for getting good 3D images [14].

2.3 Calibration

Sensor calibration is important for achieving error-free measurement against noise. Linearly deviated values between calibrated and uncalibrated sensors are error levels. Small deviation values indicate calibration and testing datasets that match equally. A distance sensor is sensitive and has the highest possibility of receiving errors in measurement data [15]. The suggestion of calibrating without using ground-truth information is by moving an uncalibrated and calibrated sensor simultaneously that points to a fixed target on a linear line, but calibrating a distance sensor using a ground-truth device gives an accurate measurement value, nevertheless, it is tedious and expensive. Furthermore, calibrating terrestrial robots using ground-truth data is even unrealistic, because distance sensors are non-linear and heteroscedasticity [16]. Correlation coefficient analysis will determine the appropriate selection of a distance sensor by measuring distances using a sensor mounted on a vehicle at a constant speed to detect the distances, and that consequently measures both sensors' performance. The objects; like cardboard, paper, sponge, wood, plastic, rubber and tile as the obstacles to determining the capability of the distance sensor's accuracy. The ultrasonic sensor detects different sets of materials, but an IR sensor detects certain types of materials. Furthermore, the present supervise machine learning algorithms contributing to the selection of a suitable distance sensor [17].

2.4 Sensor Application

2D LiDAR is suitable for mapping 3D impression since the 3D scanner is expensive but not suitable for all different applications, especially automation driving system that needs higher detection range to build a real-time scanning system. 2D LiDAR is suitable for indoor like the moving robot in their dedicated zone only needs to use a cost-effective scanner. Secondly, 2D LiDAR has a customizable field of view (FOV) and angular resolution. However, the 2D LiDAR movement is giving an error dataset when scanning at lower than 1Hz. To overcome the resolution issue, extrapolation techniques and machine learning algorithms are applied to reduce the shortfall effects in cloud point data when rotating a 2D LiDAR scanner. Furthermore, in the future 3D LiDAR will be much cheaper, but 2D LiDAR will be available if the cost is competitive to support low-cost application developments [18]. There are four common scanning methods, which are opto-mechanical, electromechanical,

micro-electromechanical system (MEMS) and solid-state. The electromechanical type is considered suitable, especially the MEMS stands out as the best because of its size, weight and consuming low energy. The solid-state is robust with a good field of view (FOV) and scanning rates, therefore research and industries use more in their experiments and products. The low-cost 3D LiDAR is relatively cheap but not recommended for fast rate requirements [19].

2.5 Sensor Detection Issues

Laser shadowing occurs when using LiDAR because of its Line-of-Sight (LOS) data, therefore airborne laser hybrid with LiDAR mounted on a tripod has been suggested for generating a fusion dataset that provides accurate measurements. The LiDAR sensor mounted on a tripod is confirmed giving accurate geometrical data of all surfaces. The fusion dataset from the airborne laser and LiDAR transformed to cartesian representation using a proprietary software, Optech which has features like built-in filters and different data representation [20]. LiDAR has been there ever since the 1960s but permeated during the introduction of automation systems for agriculture and robotics. LiDAR is suitable for calculating distances and representing scanned data to 3D digital impressions. The LiDAR's wavelength variations at reflection time measure the distance values. Therefore, transmitting lights calculates differences, so the equation below shows the distance formula Eq. (1) [21].

$$D = c(\frac{\Delta T}{2}) \tag{1}$$

D = The distance of the object
c = Speed of light
Δ = Time required by the light to travel

To acquire 3D coordinates of a LiDAR, the initial point of detection refers to the consequence points until the last point of the cloud. The final 3D reconstruction XYZ consists of the LiDAR horizontal angle, radial distance, motor vertical angle, and the distance value between the cloud points. The points translation of P0 to P1, P1 to P2, and, consequently, until the cloud's final point will transform from 2D to 3D view. Generally, 2D representation is transformed into 4x4 dimension matrix and respective equation Eq. (2);

$$T_p = R_x \times R_y \times R_z \times T \tag{2}$$

R_x , R_y and R_z represent the rotational matrix of the x-axis, y-axis and z-axis. The final 4x4 matrix elements consist of the XYZ axis rotational points, and the last column is the distance readings. The 3D construction is detected with noise, but removed with a filter. The illumination is affecting incident angles and causing outrange values. Compared to indoor measurement accuracy, outdoor measurements are affected due to sunlight rays [22].

3. Methodology

The proposed scanning method consists of testing sensors to nominate a suitable distance sensor for detecting objects on a shelf, followed by the scanner design for recording spherical coordinates, methods for tackling missing cloud points during scanning, and conversion of spherical to cartesian coordinates.

i. Sensor testing and validation

Distance sensors like Infrared (IR), Ultrasonic (US) and Light Detection and Ranging (LiDAR) have been tested and validated to select a suitable sensor in a rotating scanner system for harvesting spherical coordinates consisting of azimuth angle, elevation angle and distances [23-26]. A testing sensor was moved step by step towards a static object located at a distance. Each sensor measurement was compared and cross-validated to the readings obtained from a laser distance meter and a distance measuring tape. The selected sensor was mounted on a scanner to record distances of obstructing objects and the free spaces in a shelf tier. Figure 1 shows an experimental setup to record the distance of a distance sensor under test.

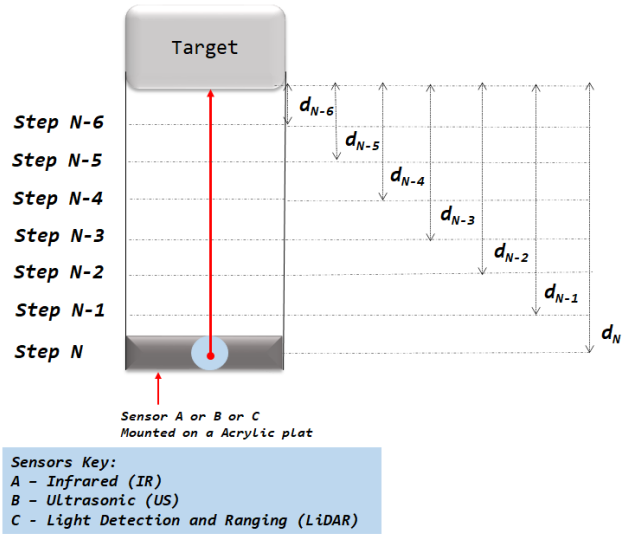

Fig. 1. Sensor distance measurement

The distance sensor was mounted firmly on an acrylic plate and moved gradually at a 5 cm distance on a step-by-step basis from N to N_{-x} towards a static target that was placed at a distance.

ii. Scanner System Design

The scanner has a microcontroller to automatically record the spherical coordinates. Figure 2 shows a LiDAR sensor and two servo motors connected to a controller for manoeuvring the scanner in a designated pattern (Figure 4). Figure 3 illustrates the parts in a scanner system, that has two integrated servo motors with a mounting bracket to mount a distance sensor, and a base plate at the bottom of the horizontal servo motor for mounting on a tripod. This complete cost-effective scanner design was made up of servo motors, a LiDAR sensor and a tripod.

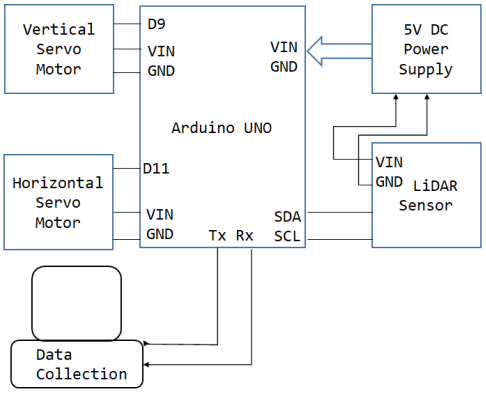

Fig. 2. LiDAR sensor and servo motors connection

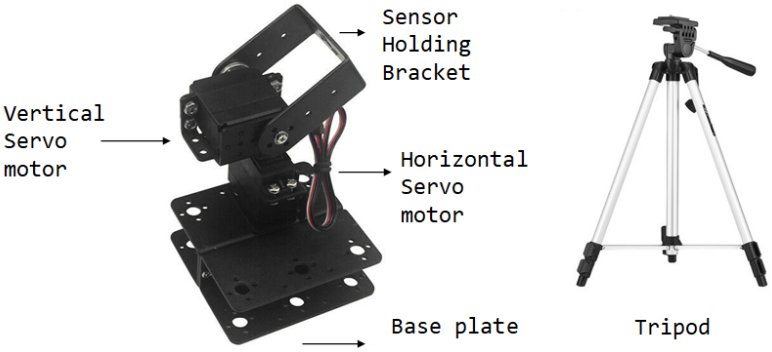

Fig. 3. Proposed integrated scanner design

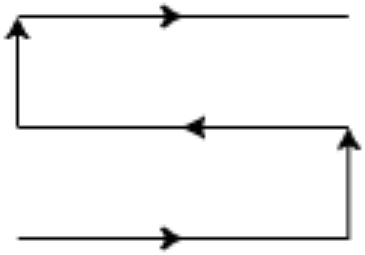

Fig. 4. Scanner manoeuvring path

iii. Mis-Matching Cloud Point Data

Figure 5 shows the harvesting of the spherical dataset from the scanner. Although LiDAR was selected for scanning distances, outliers, blunders or missing data are still presented in CPD datasets. Thus, the scanner needs a mismatched data handler when recording the spherical coordinates. Data outliers and inconsistencies happen due to the effects like vibrations, different light intensities and temperature radiation.

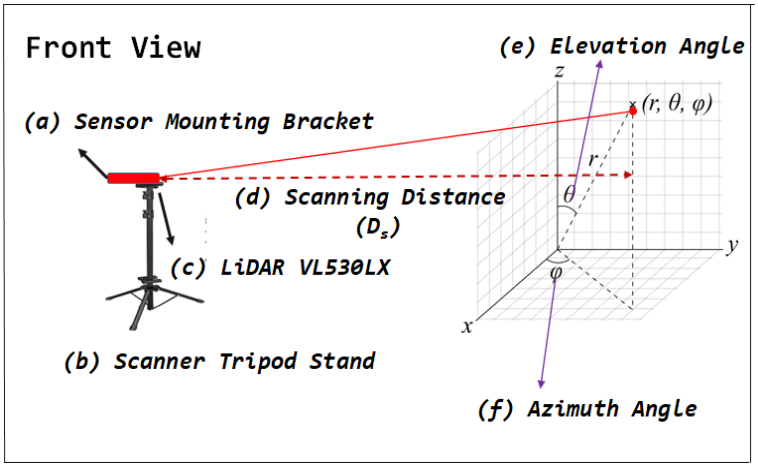

Fig. 5. Harvesting spherical data coordinates

iv. Spherical to Cartesian Coordinates

To convert spherical to cartesian coordinates, Eq. (3), Eq. (4) and Eq. (5) applied with the values from radius, azimuth and elevation in the dataset to determine x, y and z coordinates.

$$x = r \cos \varphi \sin \Theta \tag{3}$$

$$y = r \cos \varphi \cos \Theta \tag{4}$$

$$z = r \sin \varphi \tag{5}$$

4. Implementation

This section explains the implementation of sensor selection, harvesting of spherical coordinates and preprocessing of the CPD dataset. Figure 6 shows the steps to determine measurement error between a distance sensor and ground truth devices, which with using the laser meter and measuring tape in a straight line, ranging between 0 to 60 cm.

i. Selecting Distance Sensor

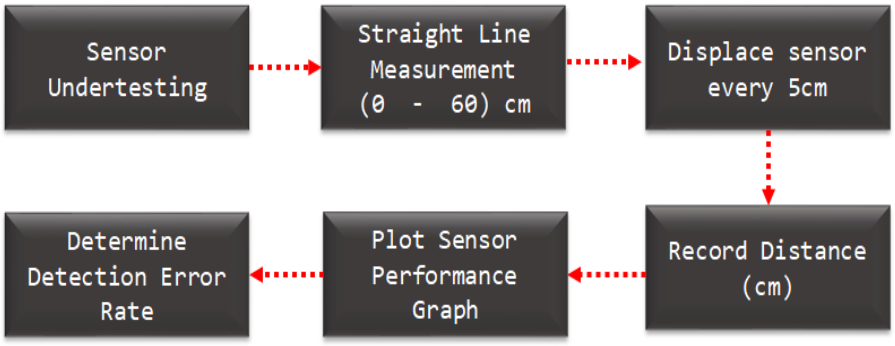

Fig. 6. Sensor testing process flow

The VL53L0X LiDAR sensor harvests the CPD dataset based on the control system process flow that is illustrated in Figure 7. The scanner rotates at 50ms to record the

radius (r), elevation (ɵ) and azimuth (ϕ) angles as the pattern shown in Figure 3. The scanner operation shown in Figure 5, is operated according to the pre-set manoeuvring path from the beginning until the finish and returns to the centre origin of the x-axis.

ii. Harvesting LiDAR Sensor Dataset

When a vertical motion was elevated by 1^{o}, consequently horizontal motion started 1^{o} displacement to capture spherical coordinates. These processes repeated until the maximum elevation angles were achieved. The scanner stopped scanning automatically, and the spherical dataset was saved for further process using MATLAB. Sometimes during scanning, the LiDAR sensor misses detections and records either zero or out-range.

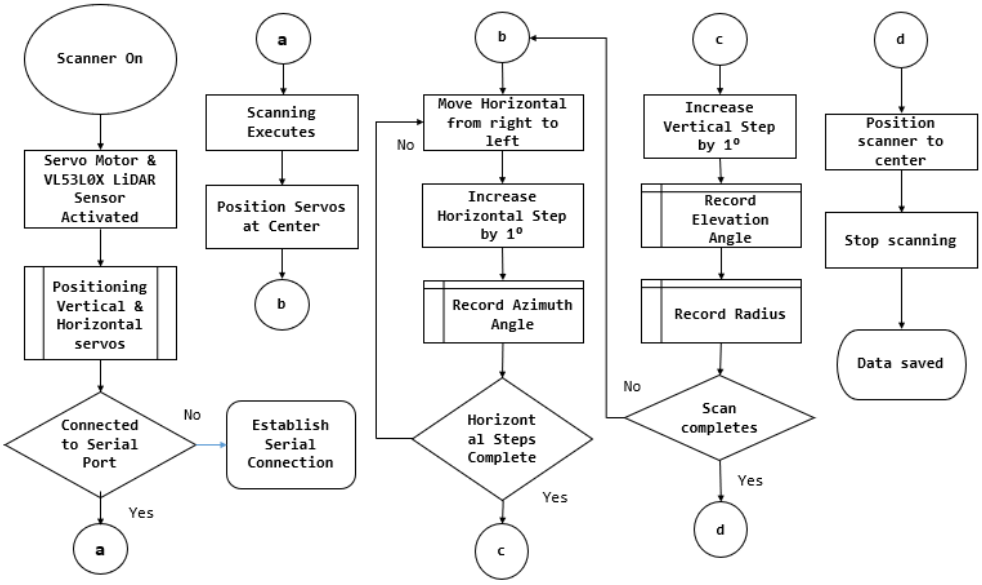

Fig. 7. Scanner Control System Process Flow

iii. Data Pre-processing Strategies

a) Avoiding Data Mis-Match

The controller detected and stored temporarily ten elements of an array, and calculated averages from the first five valid readings. The servo motor's rotation speed does influence the detection of LiDAR CPD. Even though a LiDAR sensor can detect the farthest distances, a detection cloud slips due to the rotational motion of the servo motor. Therefore, as shown in Figure 9, an experiment was modelled to collect CPD when the servo motor rotated at various speed delays at 50ms, 125ms, 250ms and 500ms.

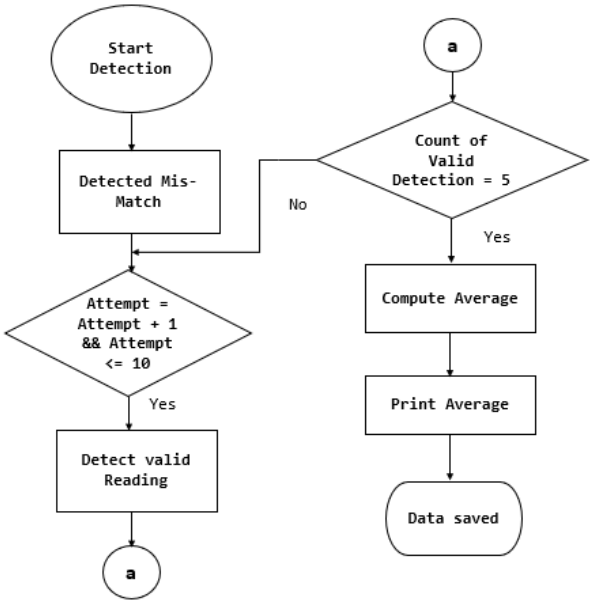

Fig. 8. Mis-match handler

b) Handling Scanner Motion Speed

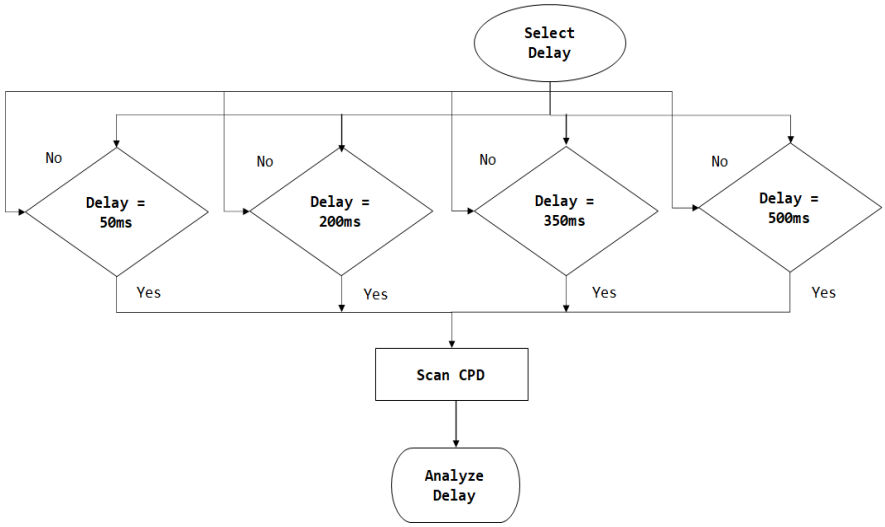

Fig. 9. Analysis of servo motion delay

As shown in Figure 10, Pearson correlation analysis and linear regression were conducted on the data between the values 50ms and 125ms, 250ms and 500ms.

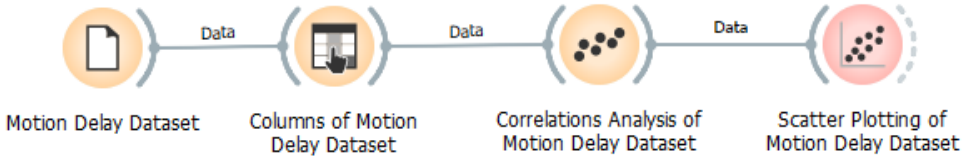

Fig. 10. Pearson correlation and regression line analysis

Figure 11 shows two important variables to determine a cartesian coordinate, which is a distance of a CPD and the armature distances, which are denoted as d and d_a. The armature distance d_a is the

length of the mounting bracket from the origin of the servo motor location. The Eq. (1), Eq. (2) and Eq. (3) were deduced to form Eq. (6), Eq. (7), Eq. (8) and Eq. (9). These expressions were programmed in MATLAB based on the steps shown in Figure 11 to determine the cartesian coordinates of the CPD.

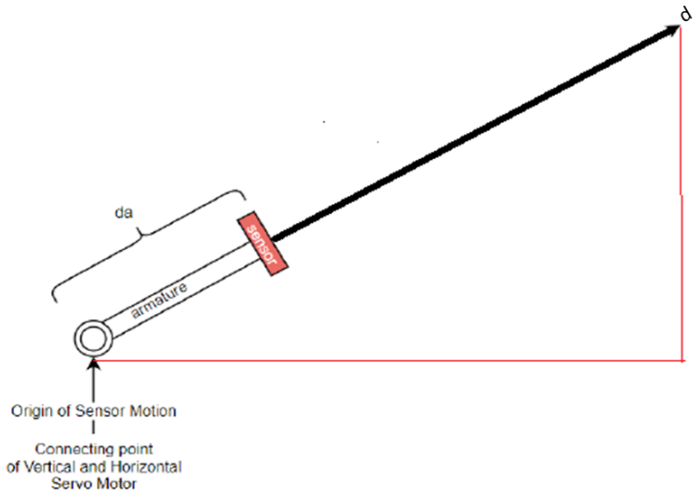

Fig. 11. Sensor armature (d_a) and distance point (d)

$$z = d \times \sin\ (\theta_V - \theta_d) \tag{6}$$

$$hc = d \times \cos\ (\theta_V - \theta_d) \tag{7}$$

$$x = hc \times \cos\ (\theta_H) \tag{8}$$

$$y = hc \times \sin\ (\theta_H) \tag{9}$$

where,

Variables	Description
d	Sensor captured distance
d_a	Sensor armature distance
h_c	The horizontal component of distances
θ_v	Sensor vertical angle
θ_d	Sensor declination angle
θ_H	Sensor horizontal angle

Figure 12 shows an overall implementation for converting a spherical to a cartesian coordinate. A lookup table stored the spherical and cartesian coordinates to use for computing space volume rate. The lookup table consists of vertical, horizontal, distances, x, y and z coordinates. Since the scanner was placed in the middle front of the x-axis, the cartesian coordinates appeared in both positive and negative quadrants. Each negative value in the x and z axis were substituted with the minimum positive value of the respective axis, so that the coordinates appeared in the positive quadrant, and the negative y-axis value was kept to zero.

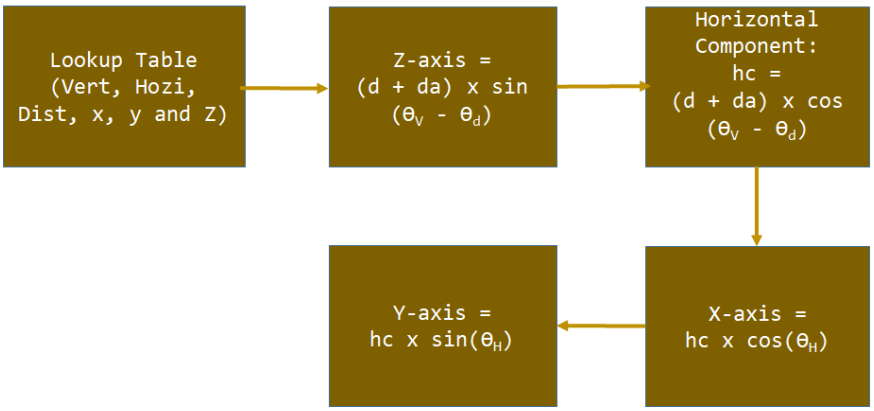

Fig. 12. Spherical to cartesian conversion steps

The vertical servo motor has to rotate from zero level position; therefore, Θ_d represents the zero-level position. However, tilted projecting was caused by Θ_d, as in Figure 13 (a). To correct the titling effects, Θ_d was deducted in conversion to Eq. (4) and Eq. (5), and the projection outcome was shown in Figure 13 (b).

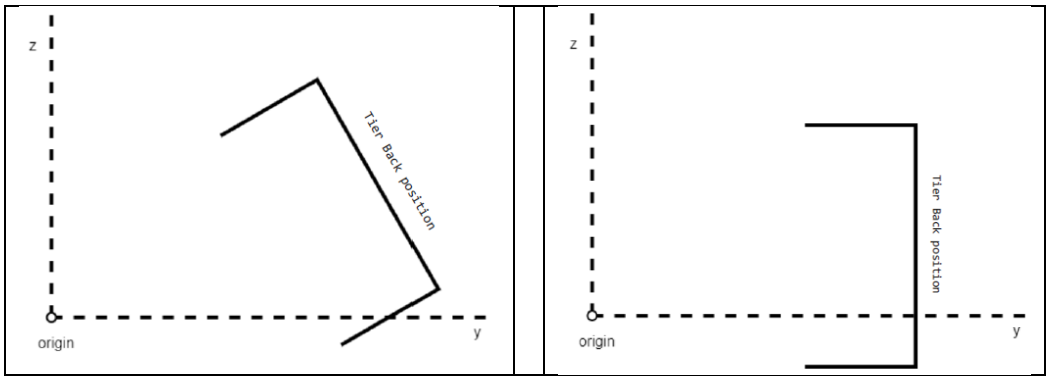

Fig. 13. (a). θ_d projection effect, (b). Projection effect after removing (θ_d)

5. Results

This study applied LiDAR as the scanner to measure the field of view (FOV) distances as the LiDAR sensor has a narrow laser beam signal with lesser refraction comparable to the ultrasound sensor, which is a radar wave in a canonical pattern that emits to detect obstacles. Capturing cloud point data (CPD) in FOV is challenging when a scanner rotates at half or full cycle. There is a high possibility of losing a detection point due to rotating speed, unavoidable mechanical vibration and surrounding changes. A code snippet shown in Figure 14, implemented to determine an average of five successive readings from the LiDAR sensor. The purpose of this code was to detect and register valid cloud point data in a dataset to determine the unutilised space. The motion delay controlled the rotational speed of two servo motors.

```
const int avg_attempts = 5;
const int avg_max_samples = 10;
Adafruit_VL53L0X lox = Adafruit_VL53L0X();

float measureAverageDistance(int attempt, int max_samples) {
  VL53L0X_RangingMeasurementData_t measure;
  long int sum = 0;
  float count = 0;
  double avg = 0;
  int i = 0;

  while ((i < max_samples) && (count < attempt)) {
    lox.rangingTest(&measure, false); // pass in 'true' to get debug data printout!
    if ((measure.RangeStatus != 4) && (measure.RangeMilliMeter > 0)) {
      sum += measure.RangeMilliMeter;
      count++;
    }

    i++;

  }

  if (count > 0) {
    avg = sum / count;
  }
  return avg;
}
```

Fig. 14. Snipnet of Mismatch Handler

Figure 15, Figure 16 and Figure 17 show scatter plotting of distance data with regression line to compare 50ms distance dataset with 125ms, 250ms and 500ms datasets. Supportively, Pearson correlation analysis in Table 1 determines the comparison between the delays. There was no significance between the delays from scatter plots and Pearson correlation analysis, therefore lowest motion delay, 50ms is suitable for scanning at higher speed. Finally, a scanner was developed using a tripod, low power, durable servo motors and a small lightweight LiDAR sensor.

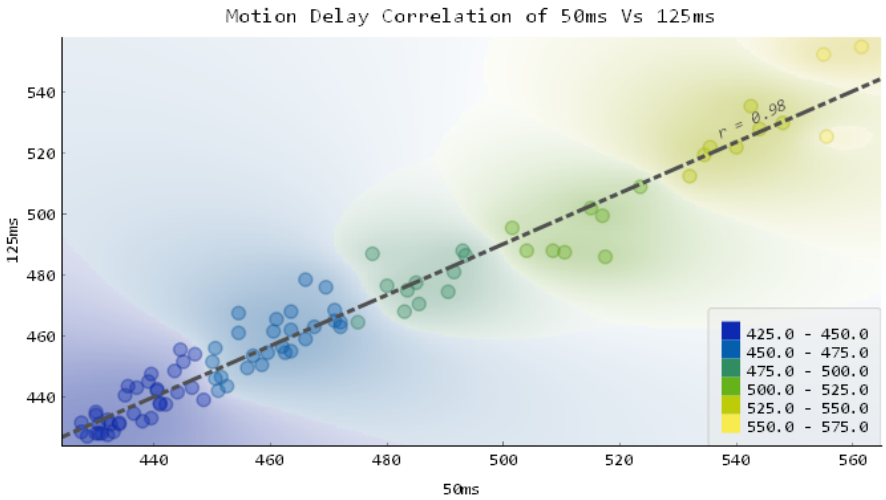

Fig. 15. Linear Regression Comparison of 50ms with 125ms

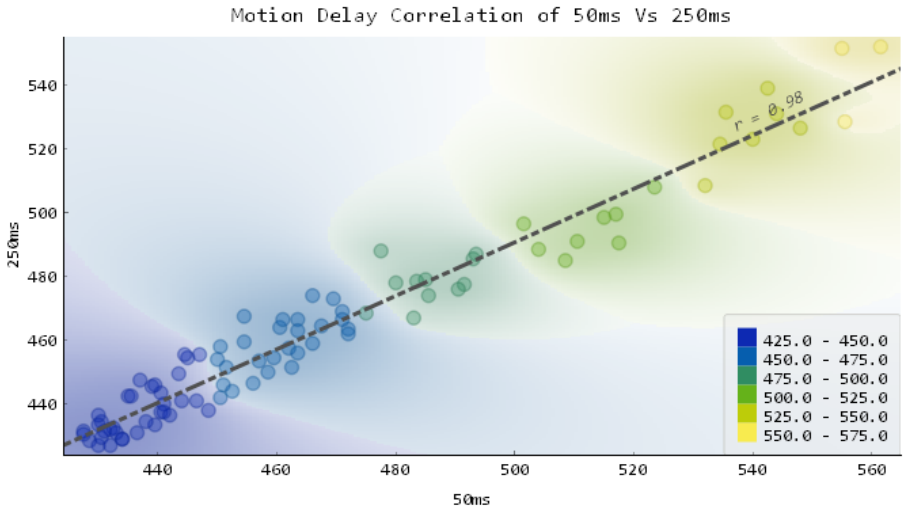

Fig. 16. Linear Regression Comparison of 50ms with 250ms

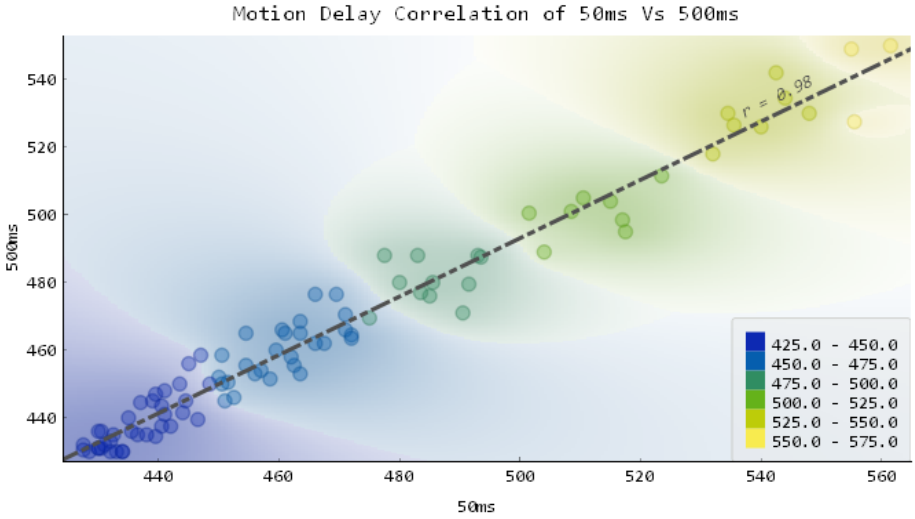

Fig. 17. Linear Regression Comparison of 50ms with 500ms

Table 1
Pearson Correlation Data Analysis

Delays (s)	50×10^{-3}	125×10^{-3}	250×10^{-3}	500×10^{-3}
50×10^{-3}	1.000	0.977	0.977	0.983
125×10^{-3}	0.977	1.000	0.997	0.990
250×10^{-3}	0.977	0.977	1.000	0.999
500×10^{-3}	0.983	0.990	0.990	1.000

Figure 18 shows an impression of 3D cartesian coordinates of a shelf tier with the object inside of the shelf tier, and the labels indicated areas with and without objects. The scanner is positioned at the middle position of a tier shelf. The cartesian coordinates appeared in positive and negative quadrants, shown in Figure 18 (a), and Figure 18 (b) has shown negative coordinates translation to the positive region of cartesian. The coordinates translation is important to compute the percentage of unutilised space in a shelf tier.

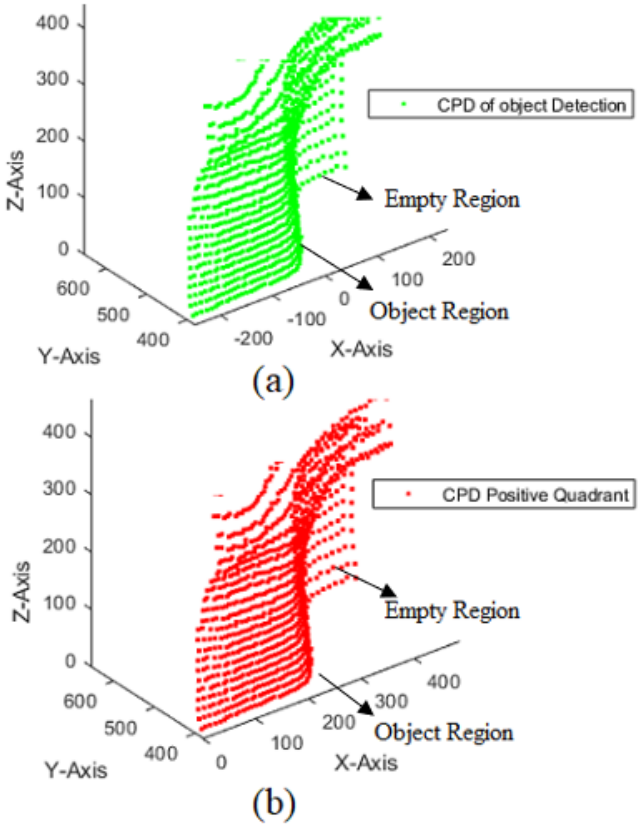

Fig. 18. 3D of An Object and Empty Space

6. Conclusions

The scanner design incorporated a function that avoids data discrepancy in the dataset. The 50ms motor rotational speed increases the scanning speed and efficiently harvests data to produce the 3D impression from cartesian coordinates. The experimental results of this study have confirmed that the proposed scanner design is suitable for obtaining the CPD of a shelf tier. The data recorded from LiDAR has data loss, therefore extrapolation needs to complete the hidden zone to produce an accurate 3D impression. In future work, machine learning algorithms such as support vector machine, (SVM) or K-Nearest Neighbour (KNN) models will be applied to develop a sensory self-healing model to countermeasure outliers or loss data that either extrapolate or modify data value in the dataset to estimate the availability of the free space in a shelf tier.

Acknowledgement

This research was funded by a grant from the Ministry of Higher Education of Malaysia (FRGS Grant FRGS/1/2018/TK03/SEGI/02/1).

References

[1] de Koster, René BM. "Automated and robotic warehouses: developments and research opportunities." *Logistics and Transport* 38, no. 2 (2018): 33-40. https://doi.org/10.26411/83-1734-2015-2-38-4-18

[2] Li, Li, and Zhuxi Chen. "Hungarian-based heuristics for single-machine flow-rack AS/RS with determined storage and retrieval locations." In *Proceedings of the 3rd International Conference on Computer Science and Application Engineering*, pp. 1-7. 2019. https://doi.org/10.1145/3331453.3361669

[3] McCrea, B. "Racking and Shelving Market Reaching New Highs." *Modern Materials Handling,* (2019).

[4] Caltagirone, Luca, Mauro Bellone, Lennart Svensson, and Mattias Wahde. "LIDAR–camera fusion for road detection using fully convolutional neural networks." *Robotics and Autonomous Systems* 111 (2019): 125-131. https://doi.org/10.1016/j.robot.2018.11.002
[5] Liu, Xiulong, Jiannong Cao, Yanni Yang, and Shan Jiang. "CPS-based smart warehouse for industry 4.0: A survey of the underlying technologies." *Computers* 7, no. 1 (2018): 13. https://doi.org/10.3390/computers7010013
[6] Rennie, Colin, Rahul Shome, Kostas E. Bekris, and Alberto F. De Souza. "A dataset for improved rgbd-based object detection and pose estimation for warehouse pick-and-place." *IEEE Robotics and Automation Letters* 1, no. 2 (2016): 1179-1185. https://doi.org/10.1109/LRA.2016.2532924
[7] Cho, Hyunggi, Young-Woo Seo, BVK Vijaya Kumar, and Ragunathan Raj Rajkumar. "A multi-sensor fusion system for moving object detection and tracking in urban driving environments." In *2014 IEEE International Conference on Robotics and Automation (ICRA)*, pp. 1836-1843. IEEE, 2014. https://doi.org/10.1109/ICRA.2014.6907100
[8] Wei, Pan, Lucas Cagle, Tasmia Reza, John Ball, and James Gafford. "LiDAR and camera detection fusion in a real-time industrial multi-sensor collision avoidance system." *Electronics* 7, no. 6 (2018): 84. https://doi.org/10.3390/electronics7060084
[9] Nada, Ayat, Samia Mashelly, Mahmoud A. Fakhr, and Ahmed F. Seddik. "Effective fast response smart stick for blind people." In *Proceedings of the second nternational Conference on Advances in bio-informatics and environmental engineering–ICABEE*. 2015.
[10] Pavithra, B. G., P. Siva Subba Rao, A. Sharmila, S. Raja, and S. J. Sushma. "Characteristics of different sensors used for Distance Measurement." *International Research Journal of Engineering and Technology (IRJET)* 4, no. 12 (2017): 698-702.
[11] Suryanto, Eka Dodi, Hendrik Siagian, Despaleri Perangin-Angin, Rahayu Sashanti, and Suthes Yogen. "Design of automatic mobile trolley using ultrasonic sensors." In *Journal of Physics: Conference Series*, vol. 1007, no. 1, p. 012058. IOP Publishing, 2018. https://doi.org/10.1088/1742-6596/1007/1/012058
[12] He, Qingdong, Zhengning Wang, Hao Zeng, Yi Zeng, and Yijun Liu. "Svga-net: Sparse voxel-graph attention network for 3d object detection from point clouds." In *Proceedings of the AAAI Conference on Artificial Intelligence*, vol. 36, no. 1, pp. 870-878. 2022. https://doi.org/10.1609/aaai.v36i1.19969
[13] Mohammad, Tarek. "Using ultrasonic and infrared sensors for distance measurement." *World academy of science, engineering and technology* 51 (2009): 293-299.
[14] Daud, Siti Asmah, Nasrul Humaimi Mahmood, P. L. Leow, and Fauzan Khairi Che Harun. "The used of infrared sensor for 3D image reconstruction." *J. Teknol* 73, no. 3 (2015): 127-132. https://doi.org/10.11113/jt.v73.4257
[15] Haitjema, Han. "The calibration of displacement sensors." *Sensors* 20, no. 3 (2020): 584. https://doi.org/10.3390/s20030584
[16] Alhashimi, Anas, Damiano Varagnolo, and Thomas Gustafsson. "Calibrating distance sensors for terrestrial applications without groundtruth information." *IEEE Sensors Journal* 17, no. 12 (2017): 3698-3709. https://doi.org/10.1109/JSEN.2017.2697850
[17] Adarsh, S., S. Mohamed Kaleemuddin, Dinesh Bose, and K. I. Ramachandran. "Performance comparison of Infrared and Ultrasonic sensors for obstacles of different materials in vehicle/robot navigation applications." In *IOP Conference Series: Materials Science and Engineering*, vol. 149, no. 1, p. 012141. IOP publishing, 2016. https://doi.org/10.1088/1757-899X/149/1/012141
[18] Bi, Shusheng, Chang Yuan, Chang Liu, Jun Cheng, Wei Wang, and Yueri Cai. "A survey of low-cost 3D laser scanning technology." *Applied Sciences* 11, no. 9 (2021): 3938. https://doi.org/10.3390/app11093938
[19] Raj, Thinal, Fazida Hanim Hashim, Aqilah Baseri Huddin, Mohd Faisal Ibrahim, and Aini Hussain. "A survey on LiDAR scanning mechanisms." *Electronics* 9, no. 5 (2020): 741. https://doi.org/10.3390/electronics9050741
[20] Iavarone, A., and D. Vagners. "Sensor fusion: Generating 3D by combining airborne and tripod-mounted LIDAR data." In *Proceedings of the International Workshop on Visualization and Animation of Reality-Based 3D Models*, vol. 34. 2003.
[21] Suharsono, Judi, and Sulis Candra. "Murabaha in Sharia Added Value, an Effort to Increase Probolinggo Shallot Farmers' Economic Scale and Spirituality." *Available at SSRN 2596062* (2013). https://doi.org/10.2139/ssrn.2596062
[22] Murcia, Harold F., Maria Fernanda Monroy, and Luis Fernando Mora. "3D scene reconstruction based on a 2D moving LiDAR." In *Applied Informatics: First International Conference, ICAI 2018, Bogotá, Colombia, November 1-3, 2018, Proceedings 1*, pp. 295-308. Springer International Publishing, 2018. https://doi.org/10.1007/978-3-030-01535-0_22
[23] Ayrey, Elias, and Daniel J. Hayes. "The use of three-dimensional convolutional neural networks to interpret LiDAR for forest inventory." *Remote Sensing* 10, no. 4 (2018): 649. https://doi.org/10.3390/rs10040649
[24] Kovács, György, and Szilvia Nagy. "Ultrasonic sensor fusion inverse algorithm for visually impaired aiding applications." *Sensors* 20, no. 13 (2020): 3682. https://doi.org/10.3390/s20133682

[25] Adarsh, S., S. Mohamed Kaleemuddin, Dinesh Bose, and K. I. Ramachandran. "Performance comparison of Infrared and Ultrasonic sensors for obstacles of different materials in vehicle/robot navigation applications." In *IOP Conference Series: Materials Science and Engineering*, vol. 149, no. 1, p. 012141. IOP publishing, 2016. https://doi.org/10.1088/1757-899X/149/1/012141

[26] STMicroelectronics, VL53L1X. "A new generation, long distance ranging Time-of-Flight sensor based on ST's FlightSense™ technology." *VL53L1X Datasheet* (2018).